Published for SISSA by Springer

Received: *September 16, 2014*
Revised: *October 13, 2014*
Accepted: *November 11, 2014*
Published: *December 2, 2014*

Vortex solutions of an Abelian Higgs model with visible and hidden sectors

Paola Arias[a] **and Fidel A. Schaposnik**[b,1]

[a] *Departamento de Física, Pontificia Universidad Católica de Chile, Casilla 306, Santiago 22, Chile*

[b] *Departamento de Física, Universidad Nacional de La Plata, Instituto de Física La Plata, C.C. 67, 1900 La Plata, Argentina*

E-mail: paola.arias@fis.puc.cl, fidel@fisica.unlp.edu.ar

Abstract: We study vortex solutions in a theory with dynamics governed by two weakly coupled Abelian Higgs models, describing a hidden sector and a visible sector. We analyze the radial dependence of the axially symmetric solutions constructed numerically and discuss the stability of vortex configurations for different values of the model parameters, studying in detail vortex decay into lower energy configurations. We find that even in a weak coupling regime vortex solutions strongly depend on the parameters of both the visible and hidden sectors. We also discuss on qualitative grounds possible implications of the existence of a hidden sector in connection with superconductivity and dark matter (dark strings).

Keywords: Spontaneous Symmetry Breaking, Topological Strings

ArXiv ePrint: 1407.2634

[1] Also at CICBA.

doi:10.1007/JHEP12(2014)011

JHEP12(2014)011

Contents

1 Introduction 1

2 The model 2

3 One unbroken U(1) symmetry 5

4 Numerical results 7
- 4.1 Variational analysis 7
- 4.2 Changing χ 8
- 4.3 Changing the ratio $e_h/e \equiv e_r$ 9
- 4.4 Radial dependence of fields 12
- 4.5 Vortex decay into elementary configurations 14

5 The fields behavior in connection with superconductivity 15

6 Summary and discussion 19

A Asymptotic behavior of the radial fields 21

1 Introduction

Models with vector bosons and scalars in a hidden sector naturally arise in supersymmetric extensions of the standard model as well as in superstring phenomenological studies. They have also cosmological implications concerning gravitational wave production and dark matter abundance (see [1] and references therein). Regarding this last issue, the hidden massive gauge boson could play the role of dark matter [2, 3] or could be the messenger between the visible and dark sectors [4]. Also, when the hidden sector has a U(1) symmetry the corresponding gauge boson may have a very weak kinetic interaction with photons in the visible sector [5, 6], which could lead to observable effects in experiments like those on light shining through the wall, laser polarization and strong electromagnetic fields [1]. Furthermore, when the hidden U(1) gauge symmetry is spontaneously broken the classical field equations exhibit the well-honored Nielsen-Olesen vortex solutions that can play the role of dark strings in an astrophysical context, as proposed in [7]–[10].

In view of the various areas in which the hidden sector could play an important role in explaining physical phenomena, it is of interest to undertake the detailed study that we present in this work where we construct vortex solutions of two Abelian Higgs models associated to visible and hidden sectors weakly coupled through a gauge mixing interaction. In particular, we analyze how the effects of the hidden sector depend not only on the strength of the mixing between the two U(1) gauge bosons but also on the relative strength

JHEP12(2014)011

of the gauge coupling constants and on the scalar potentials parameters including the case in which one of the U(1) gauge symmetry remains unbroken. Another relevant subject that we analyze concerns vortex decay. In the ordinary Abelian Higgs model vortex configurations with $n > 1$ units of magnetic flux could decay into elementary ($n = 1$) vortices depending on the value of the Landau parameter [11]. We study this issue for configurations in which both hidden and visible vortices exist, and determine how the mixing affects the decay scenario.

The plan of the paper is as follows: we introduce the model in section 2, extending the Nielsen-Olesen ansatz to include the hidden sector, leading to a coupled system of four radial field equations. In section 3 we consider the case in which the visible sector gauge symmetry is unbroken and discuss analytically how the spontaneous breaking of the hidden sector gauge symmetry is communicated to the visible sector. Then, in section 4 we analyze numerically the case in which both the visible and hidden sectors gauge symmetries are broken studying the dependence of the vortex solutions on the gauge mixing parameter (section 4.2) and on the gauge coupling constants (section 4.3) using both a variational approach and a shooting method. Vortex decay is studied in section 5 and a discussion of the relevance of the model in connection with superconductivity is presented in section 6. Section 7 gives a summary and discussion of our results.

2 The model

We consider a model with two U(1) gauge fields, A_μ and G_μ, each one coupled to complex scalars, ϕ and ψ respectively, with dynamics governed by the following Lagrangian in $3+1$ space-time dimensions

$$\mathcal{L} = -\frac{1}{4}F_{\mu\nu}F^{\mu\nu} - \frac{1}{2}|D_A^\mu\phi|^2 - V(\phi) - \frac{\chi}{2}F_{\mu\nu}G^{\mu\nu} - \frac{1}{4}G_{\mu\nu}G^{\mu\nu} - \frac{1}{2}|D_G^\mu\psi|^2 - V(\psi). \quad (2.1)$$

Here

$$F_{\mu\nu} = \partial_\mu A_\nu - \partial_\nu A_\mu \,, \qquad G_{\mu\nu} = \partial_\mu G_\nu - \partial_\nu G_\mu \quad (2.2)$$

$$D_A^\mu\phi = (\partial^\mu - ieA^\mu)\phi \,, \qquad D_G^\mu\psi = (\partial^\mu - ie_h G^\mu)\psi \quad (2.3)$$

and $V(\phi), V(\psi)$ are given by

$$V(\phi) = \frac{\lambda}{4}\left(|\phi|^2 - \phi_0^2\right)^2 \,, \qquad V(\psi) = \frac{\lambda_{\rm h}}{4}\left(|\psi|^2 - \psi_0^2\right)^2 \quad (2.4)$$

In our convention the set of fields A_μ and ϕ belong to the visible sector, while G_μ and ψ belong to the hidden one. The strength of the mixing between the two gauge fields is parameterized by χ which could be either positive or negative. Theoretical and observational constraints seem to favor at present that this parameter is small (natural values of the kinetic mixing from string theory can be found in [12]; for recent observational constraints on hidden photons see [13]). Although in principle χ is a free parameter, we show in the appendix that consistency of boundary conditions leading to the existence of finite energy vortex solutions requires $|\chi|^2 < 1$.

JHEP12(2014)011

We are interested in static configurations with $A_0 = G_0 = 0$ for which the energy density $\mathcal{E}$ associated to Lagrangian (2.1) takes the form

$$\mathcal{E} = \frac{B_i B_i}{2} + \frac{B_{hi} B_{hi}}{2} + \chi B_i B_{hi} + \frac{1}{2}|D_A^\mu \phi|^2 + \frac{1}{2}|D_G^\mu \psi|^2 + V(\phi) + V(\psi). \tag{2.5}$$

with the magnetic fields of the visible and hidden sector defined as

$$B^i = \varepsilon^{ijl}\partial_j A_k \ , \quad B_h^i = \varepsilon^{ijl}\partial_j G_k. \tag{2.6}$$

Due to the choice of symmetry breaking potentials, both gauge fields acquire masses given by $m_A^2 = e^2\phi_0^2$ and $m_G^2 = e_h^2\psi_0^2$. Concerning the scalars, their masses are given by $m_\phi^2 = 2\lambda\phi_0^2$ and $m_\psi^2 = 2\lambda_h\psi_0^2$ according to the Brout-Englert-Higgs mechanism.

It will be convenient for later use to define dimensionless coordinates, coupling constants and fields according to

$$r \to r/\left(e\phi_0\right), \ \ A_i \to \phi_0 A_i, \ \ \phi \to \phi_0\phi, \ \ G_i \to \phi_0 G_i, \ \ \psi \to \phi_0\psi. \tag{2.7}$$

With this, the energy per unit length E/ℓ in the z direction, and with $A_z = G_z = 0$, reads

$$\begin{aligned}\frac{E}{\ell} = \phi_0^2 \int d^2x \Big\{ &\frac{B_i B_i}{2} + \frac{B_{hi} B_{hi}}{2} + \frac{1}{2}\left|\partial_i\phi - iA_i\phi\right|^2 \\ &+\frac{1}{2}\left|\partial_i\psi - ie_r G_i\psi\right|^2 + \chi B_i B_{hi} + V(|\phi|) + V(|\psi|)\Big\} \equiv \phi_0^2 \int d^2x\, \tilde{\mathcal{E}},\end{aligned} \tag{2.8}$$

where $e_r = e_h/e$ and ℓ defines the length scale, $\ell = 1/e\phi_0$. The symmetry breaking potentials are now given by

$$V(|\phi|) = \frac{\kappa^2}{8}\left(|\phi|^2 - 1\right)^2, \quad V(|\psi|) = \frac{\beta^2 e_r^2}{8}\left(|\psi|^2 - \frac{\mu^2}{e_r^2}\right)^2. \tag{2.9}$$

Here we have defined a dimensionless parameter as $\kappa^2 = 2\lambda/e^2$, which is related to the *Landau parameter* in the Ginzburg-Landau theory of superconductivity. The parameter $\beta^2 = 2\lambda_h/e_h^2$, is its hidden analogue. Concerning the parameter μ, it corresponds to the ratio of the hidden and visible gauge vector masses, $\mu = m_G/m_A = e_r\psi_0/\phi_0$. In the ordinary Abelian Higgs model, $\kappa < 1$ corresponds to Type I superconductivity and $\kappa > 1$ to Type II superconductivity. The limiting value $\kappa = 1$ is usually called the Bogomolny point (for the ordinary Abelian Higgs model). At $\kappa = 1$ can be derived a lower bound for the energy [14, 15]. The bound is saturated whenever the gauge and scalar fields satisfy a system of coupled first order equations and the energy is then proportional to the number of quantized units of magnetic flux of the vortex solutions.

After the redefinitions stated in eq. (2.7) the visible gauge and scalar fields masses become $m_A = 1$ and $m_\phi = \kappa = \sqrt{2\lambda/e^2}$, respectively. Concerning the hidden Higgs mass, it takes the value $m_\psi = \sqrt{2\lambda_h\mu^2/e_h^2}$. We are interested in finding static axially symmetric solutions of the field equations, so it will be convenient to consider polar coordinates (r, φ, z) and search for z independent field configurations. We then propose the

JHEP12(2014)011

well-honored Nielsen-Olesen [16] ansatz both for the visible and the hidden sectors

$$\phi = \rho(r)e^{in\varphi}, \qquad A_\varphi = n\frac{\alpha(r)}{r}, \qquad A_r = 0, \qquad A_z = 0, \qquad n \in \mathbb{Z}. \tag{2.10}$$

$$\psi = p(r)e^{ik\varphi}, \qquad G_\varphi = k\frac{\gamma(r)}{e_r r}, \qquad G_r = 0, \qquad G_z = 0, \qquad k \in \mathbb{Z}. \tag{2.11}$$

Inserting this ansatz, the energy density (2.8) in terms of the redefined coordinates and parameters (2.7) takes the form

$$\begin{aligned}\tilde{\mathcal{E}} = &\frac{n^2}{2r^2}\left(\frac{d\alpha}{dr}\right)^2 + \frac{k^2}{2e_r^2 r^2}\left(\frac{d\gamma}{dr}\right)^2 + \chi\frac{nk}{e_r r^2}\frac{d\gamma}{dr}\frac{d\alpha}{dr} + \frac{1}{2}\left(\frac{d\rho}{dr}\right)^2 + \frac{1}{2}\left(\frac{dp}{dr}\right)^2 \\ &+\frac{n^2}{2r^2}(1-\alpha)^2\rho^2 + \frac{k^2}{2r^2}(1-\gamma)^2 p^2 + \frac{\kappa^2}{8}\left(\rho^2-1\right)^2 + \frac{\beta^2 e_r^2}{8}\left(p^2 - \frac{\mu^2}{e_r^2}\right)^2.\end{aligned} \tag{2.12}$$

Finite energy density requires the following behavior of fields at the origin and at infinity

$$\begin{aligned}&\rho(0) = p(0) = 0\,, \qquad \lim_{r\to\infty}\rho(r) = 1\,, \qquad \lim_{r\to\infty} p(r) = \frac{\mu}{e_r} \\ &\alpha(0) = \gamma(0) = 0\,, \qquad \lim_{r\to\infty}\alpha(r) = \lim_{r\to\infty}\gamma(r) = 1\end{aligned} \tag{2.13}$$

Using the asymptotic behavior and the fact that finite energy requires covariant derivatives for both scalars to vanish at infinity one finds that the magnetic flux in the visible and hidden sectors can be written in terms of the scalar fields in the form

$$\Phi_A = \oint_{\mathcal{C}_\infty} A_\mu dx^\mu = \frac{i}{e|\phi_0|^2}\oint_{\mathcal{C}_\infty}\phi^*\partial_\mu\phi\, dx^\mu = \frac{2\pi n}{e}\,, \quad n \in \mathbf{Z} \tag{2.14}$$

$$\Phi_G = \oint_{\mathcal{C}_\infty} G_\mu dx^\mu = \frac{i}{e_h|\psi_0|^2}\oint_{\mathcal{C}_\infty}\psi^*\partial_\mu\psi\, dx^\mu = \frac{2\pi k}{e_h}\,, \quad k \in \mathbf{Z} \tag{2.15}$$

Here the fluxes are written in terms of the original fields introduced in eqs.(2.1)–(2.4), i.e. before redefining coordinates, coupling constants and fields.

Given ansatz (2.11), the field equations for the model take the form

$$n\alpha'' + \chi\frac{k}{e_r}\gamma'' - \chi\frac{k}{e_r}\frac{\gamma'}{r} - n\frac{\alpha'}{r} - n(\alpha-1)\rho^2 = 0. \tag{2.16}$$

$$\frac{k}{e_r}\gamma'' + n\chi\alpha'' - \frac{k}{e_r}\gamma' - \chi n\frac{\alpha'}{r} - ek(\gamma-1)p^2 = 0. \tag{2.17}$$

$$\frac{1}{r}\frac{d}{dr}\left(r\rho'\right) - \frac{n^2}{r^2}(1-\alpha)^2\rho - \frac{\kappa^2}{2}\left(\rho^2-1\right)\rho = 0. \tag{2.18}$$

$$\frac{1}{r}\frac{d}{dr}\left(rp'\right) - \frac{k^2}{r^2}(1-\gamma)^2 p - \frac{\beta^2 e_r^2}{2}\left(p^2 - \frac{\mu^2}{e_r^2}\right)p = 0. \tag{2.19}$$

where the prime indicates from now on a derivative with respect to r.

Equations (2.16)–(2.19) decouple in the asymptotic regime where analytic solutions can be easily found. The asymptotic solution for $\alpha(r)$ and $\gamma(r)$ is encoded in the equation

$$\left[r\frac{d}{dr}\left(\frac{1}{r}\frac{d}{dr}\right)\right]F_\pm = \frac{1}{\sqrt{C_\pm}}F_\pm, \tag{2.20}$$

JHEP12(2014)011

where $F_\pm$ are a linear combination of α and γ and $C_\pm$ are coefficients depending on χ and μ (see appendix for details). Finite energy per unit length solutions require $\chi^2 < 1$. Thus, in order to have finite energy vortex solutions, the parameter χ - controlling the mixing between the visible and hidden sectors - should satisfy $|\chi| < 1$.

Due to the presence of the gauge kinetic mixing no first-order Bogomolny equations [14, 15] can be found when $\chi \neq 0$, except for a very particular case [8]. Evidently, if fields and parameters in the visible and the hidden sector are identified (this implying also the the number of units of magnetic flux in the ansatz), Lagrangian (2.8) becomes the same as that of the ordinary Abelian Higgs model apart from an overall factor 1/2 and a shift in the gauge coupling constant $e \to e/\sqrt{1-\chi^2}$. Hence, in this very special case one finds the usual Bogomolny equations with the Bogomolny point separating Type I and Type II superconductivities shifted accordingly, $\kappa^2 \to (1-\chi^2)\kappa^2$. We shall not discuss this case in which visible and hidden sectors become indistinguishable since it escapes the main interest of our work.

3 One unbroken U(1) symmetry

Let us start by studying the existence and stability of vortex solutions when one of the U(1) gauge groups remains unbroken. A related discussion has been presented in [8], but we include the analysis here for completeness and to highlight certain features that the model exhibits and we consider of interest.

Let us assume that the visible U(1) gauge group remains unbroken (we could have chosen the other way around as well). The simplest way to achieve this is by eliminating the visible scalar sector so that all ϕ dependent terms in Lagrangian (2.1) are absent.

The energy density then reads

$$\mathcal{E}_{\mathrm{U}(1)} = \frac{B_i B_i}{2} + \frac{B_{hi} B_{hi}}{2} + \chi B_i B_{hi} + \frac{1}{2}\left|\partial_i \psi - i e_h G_i \psi\right|^2 + V(|\psi|) \tag{3.1}$$

We now perform a redefinition of the visible magnetic field as

$$B_i = \tilde{B}_i - \chi B_{hi}, \tag{3.2}$$

the energy density $\mathcal{E}_{\mathrm{U}(1)}$ becomes

$$\mathcal{E}_{\mathrm{U}(1)} = (1-\chi^2)\frac{B_{hi} B_{hi}}{2} + \frac{\tilde{B}_i \tilde{B}_i}{2} + \frac{1}{2}\left|\partial_i \psi - i e_h G_i \psi\right|^2 + V(|\psi|). \tag{3.3}$$

Now, a redefinition of the hidden vector field, as

$$G_i = \frac{G'_i}{\sqrt{1-\chi^2}}, \tag{3.4}$$

leads to $B_{hi} = B'_{hi}/\sqrt{1-\chi^2}$. We can rewrite the energy (3.3) in terms of the new fields as

$$\mathcal{E}_{\mathrm{U}(1)} = \frac{B'_{hi} B'_{hi}}{2} + \frac{\tilde{B}_i \tilde{B}_i}{2} + \frac{1}{2}\left|\partial_i \psi - i e_{\mathrm{eff}} G'_i \psi\right|^2 + V(|\psi|), \tag{3.5}$$

where we have defined an effective coupling constant e_{eff}, for the hidden gauge field

$$e_{\text{eff}} = \frac{e_h}{\sqrt{1-\chi^2}}. \tag{3.6}$$

Let us note that in terms of the redefined fields, the energy density is the sum of two uncoupled terms: the one corresponding to the hidden sector coincides with the ordinary Nielsen-Olesen vortex energy density, while the other one is just a Maxwell term for the $\tilde{B}$ magnetic field. In this form, the energy density can be written as a sum of squares whenever coupling constants are accommodated to fulfill the Bogomolny condition

$$\begin{aligned} E/\ell = \psi_0^2 \int d^2x \frac{1}{4} \Big\{ & \left(G'_{ij} \pm \varepsilon_{ij}\left(\psi^a\psi^a - 1\right)\right)^2 + \left(D_i\psi^a \mp \varepsilon^{ab}\varepsilon_{ij}D_j\psi^b\right)^2 \\ & + 4\left(\frac{\beta_h}{2} - \frac{1}{2}\right)\left(\psi^a\psi^a - 1\right)^2 \pm \left(\varepsilon_{ij}G'_{ij} \mp \varepsilon^{ab}\varepsilon_{ij}\partial_i\left(\psi^a D_j\psi^b\right)\right) + \tilde{B}_i\tilde{B}^i \Big\}. \end{aligned} \tag{3.7}$$

Where we have moved to the dimensionless variables, $r \to r/(e_{\text{eff}}\psi_0)$, $G'_i \to G'_i\psi_0$, $\psi \to \psi\psi_0$, $\tilde{A}_i \to \psi_0\tilde{A}_i$.

The minimization of the energy is bounded from below to

$$E/\ell \geq \psi_0^2 \frac{2\pi}{e_{\text{eff}}}k, \qquad k \in \mathbb{Z}. \tag{3.8}$$

The bound is saturated when the following set of Bogomolny equations are satisfied

$$G'_{ij} = \mp\varepsilon_{ij}\left(\psi^a\psi^a - 1\right). \tag{3.9}$$

$$D_i\psi^a = \pm\varepsilon^{ab}_{ij}D_j\psi_b. \tag{3.10}$$

$$\frac{1}{2}\varepsilon_{ij}\tilde{F}_{ij} = 0. \tag{3.11}$$

Thus, the configuration of minimum energy is the one where $\tilde{B} = 0$. Going back to the original field of eq. (3.2),

$$B = -\chi B_h. \tag{3.12}$$

This result shows that even in the absence of symmetry breaking, the mixing between the visible and the hidden gauge field forces the former to form a vortex with the same winding number k as the broken gauge field hence having a quantized magnetic flux

$$\Phi = \oint_{\mathcal{C}_\infty} A_\mu dx^\mu = -\frac{\chi}{e_{\text{eff}}}2\pi k. \tag{3.13}$$

Relation (3.12) between both gauge fields implies that even in the absence of a symmetry breaking of the visible sector, the kinetic gauge mixing forces the magnetic field to have an exponential decay controlled by the hidden gauge field mass. Now, since in this case the visible magnetic field B is related to the hidden one according to $B = -\chi B_h$, its strength is diminished by the kinetic mixing parameter.

JHEP12(2014)011

This result could have interesting phenomenological implications if this model is considered as providing a mixing of hidden and visible cosmic strings in the early universe.[1]

Note that a similar topological effect for the dark and visible magnetic charge relation can take place, as described in [17, 18].

When B is an external field, $\tilde{B} = 0$ is no longer a solution, and the role of the kinetic mixing is to lower the magnetic energy of the visible sector, as noted in [8].

4 Numerical results

We shall first solve equations (2.16)–(2.19) using a simple and effective variational approach that has been shown to render the energy of vortex solutions with similar accuracy as more elaborated methods [20]. Using this approach we shall analyze the dependence of the energy on the kinetic mixing parameter χ and the gauge coupling constants. We shall also solve the field equations using an asymptotic shooting method in order to obtain accurate profiles of the gauge and scalar field vortex configurations.

4.1 Variational analysis

The idea is to combine powers of exponentials to engineer functions ρ, α, p and γ with the short- and long-distance limits imposed by conditions (2.11)

$$\begin{aligned} \alpha(r) &= \left(1 - e^{-ur}\right)^2, \qquad & \rho(r) &= 1 - e^{-hr} \\ \gamma(r) &= \left(1 - e^{-fr}\right)^2, \qquad & p(r) &= \frac{\mu}{e_r}\left(1 - e^{-vr}\right). \end{aligned} \tag{4.1}$$

Variational parameters u and f are related to the visible and hidden gauge field masses respectively while h and v are related to the masses of the visible and hidden Higgs fields. In terms of these variational parameters $\tilde{\mathcal{E}}$ takes the form:

$$\begin{aligned} \tilde{\mathcal{E}} = \frac{k^2}{2e_r^2}\Bigg(&\frac{e^{-4fr}}{r^2}\left(\mu^2\left(1-2e^{fr}\right)^2\left(1-e^{-rv}\right)^{2|k|} + 4f^2\left(e^{fr}-1\right)^2\right) \\ &+ 4v^2\mu^2 e^{-2vr}\left(1-e^{-rv}\right)^{2|k|-2}\Bigg) + \frac{n^2}{2}\Bigg(\frac{e^{-4ur}}{r^2}\Bigg((1-2e^{ur})^2\left(1-e^{-hr}\right)^{2|n|} \\ &+4u^2\left(e^{ur}-1\right)^2\Bigg) + 4h^2e^{-2hr}\left(1-e^{-hr}\right)^{2|k|-2}\Bigg) \\ &+nk\frac{4uf\chi}{e_r r^2}\left(e^{rv}-1\right)\left(e^{fr}-1\right)e^{-2r(f+u)} + \frac{\beta^2}{8}\frac{\mu^4}{e_r^2}\left(\left(1-e^{-rv}\right)^{2|k|}-1\right)^2 \\ &+\frac{\kappa^2}{8}\left(\left(1-e^{-hr}\right)^{2|n|}-1\right)^2 \end{aligned} \tag{4.2}$$

Apart from the variational parameters, there are seven free parameters which should be chosen on physical grounds: κ and β, related to the Landau parameters for both the

[1] It has been noted that cosmic strings produced during phase transitions could seed primordial magnetic fields [19]. One could think in a physical scenario where dark strings are formed during phase transition of the hidden sector, and as a consequence of the mixing, visible cosmic strings are formed, which in turn could seed a primordial magnetic field.

JHEP12(2014)011

visible and hidden sector, $e_r = e_h/e$ related to gauge coupling constants, $\mu = m_G/m_A$, the ratio of gauge field masses, χ which measures A_μ and G_μ mixing strength and n, k, the number of units of visible and hidden magnetic fluxes.

To start with and in order to test our variational approach, we have considered the case in which there is no mixing ($\chi = 0$) for which we have direct comparison with very accurate numerical results [11, 14]. We found that there is excellent agreement between those results and ours. As an example, exact $n = 1$ vortex energy per unit length at the Bogomolny point is $E/\ell = |\phi_0|^2$, while that obtained in ref. [11] using a refined variational method is $E/\ell = 1.00000|\phi_0|^2$. Concerning our simpler variational result, we obtained $E/\ell = 1.01823|\phi_0|^2$. In short, we trust the results of our variational calculation.

When the mixing between hidden and visible vector fields is so small that it can be ignored, the visible and hidden terms in the model defined by Lagrangian (2.1) decouple, and then there exist two unrelated vortex solutions with winding numbers n, k, respectively. Recall that when there is just one gauge field and one complex scalar and the Landau parameter is larger than the value it takes at the Bogomolny point, a vortex with winding number $n > 1$ decays into separated vortices (see for example [11]) and this is then true for each of the decoupled sector we refer above.

As we shall see, non negligible values of the kinetic mixing parameter χ can have great impact in the existence of vortex solutions and their behavior. This will be also the case concerning different values of the hidden gauge coupling constant e_r, and/or the hidden gauge field mass appearing in the μ parameter.

4.2 Changing χ

Here we study vortex stability as a function of the mixing parameter χ. As highlighted in the previous section, when the mixing parameter vanishes we are left with two uncoupled vortices, if their Landau parameters λ, β are greater than one and the corresponding winding numbers are greater than one, they become unstable, decaying in configurations of smaller winding numbers.

We shall show here that if the mixing is non negligible, the stability conditions change and instability could take place without requiring that both $(\lambda, \beta) > 1$ simultaneously. To see this we fix κ to the value it takes at the stability critical point (Bogomolny point [14, 15]) in the absence of mixing, when the theory reduces to two uncoupled Abelian Higgs model exhibiting independent vortex solutions. We then study the energy as a function of the hidden Landau parameter β for different values of χ.

For the case $\chi nk > 0$, our results are shown in figure 1 where we plotted the energy as a function of β for a (2,2) vortex configuration compared to twice the energy of a (1,1) configuration for different values of χ. Here our notation (n, k) stands for the energy given by equation (4.2) with winding number n of the visible sector and k of the hidden one, respectively. We see that as χ grows the value of the critical point beyond which the instability starts to move to lower and lower values of β.

When $\chi < 0$ and $nk > 0$ the situation changes drastically. One can easily see this by considering the particular limiting case $\chi \to -1$, $nk > 0$, and all other physical parameters of the visible and hidden sector identical. With this choice, the gauge fields are

JHEP12(2014)011

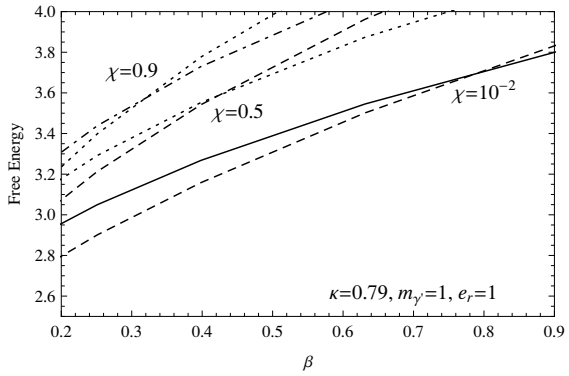

Figure 1. Stability of vortices for different values of the kinetic mixing parameter χ. We have fixed κ to the value corresponding to the critical point for the case in which there is no mixing. The rest of the parameters have been fixed to $\mu = e_r = 1$. Dashed lines correspond to the energy of a configuration $(2, 2)$ while dotted ones correspond to twice the energy of configuration $(1, 1)$. As χ increases, the critical point moves to the left.

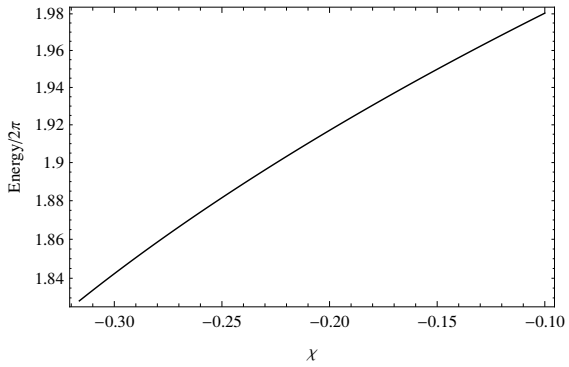

Figure 2. Energy as a function of the mixing parameter χ when $\chi < 0$. The energy decreases as χ becomes more negative. The rest of the parameters have been fixed to unity, $\mu = e_r = \kappa = \beta$=1.

indistinguishable and hence the first three terms in (2.12) cancel out and the energy will be smaller than the one in which both signs coincide. Since there is no contribution to the energy from the visible and hidden field strengths, one should expect that the total energy could become negative in some region of physical parameters and vortex-like solutions will cease to exist. Our numerical analysis confirms that this is indeed what happens, as can be seen in figure 2 where, as χ approaches to -1 the energy becomes smaller, until, in the region $\chi \gtrsim -1$ it eventually becomes negative.

If χ is still positive but $nk < 0$, i.e. the magnetic fluxes from the hidden and visible sectors have opposite signs, the variational analysis shows in figure 3 that when $nk < 0$, the free energy diminishes as χ grows approaching one. This means that it is favorable — when the mixing parameter is not negligible — to form vortices of opposite magnetic fluxes.

4.3 Changing the ratio $e_h/e \equiv e_r$

When the gauge couplings from visible and hidden sector are different the conclusion concerning the stability of vortices is similar to that in subsection (4.2). To see this let us fix the visible gauge coupling to $e = 1$ and vary the corresponding hidden one.

JHEP12(2014)011

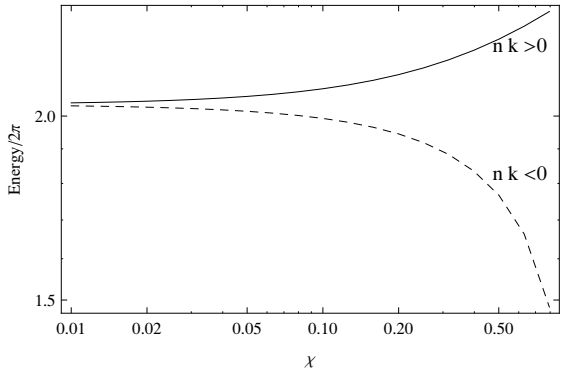

Figure 3. Energy vs. χ for a configuration with parallel fluxes, sign n = sign k, and inverted fluxes, sign $n \neq$ sign k. For higher values of χ the free energy has very different behavior for $nk > 0$, where the energy grows with χ, and $nk < 0$, where the energy diminishes as χ grows. The parameters have been fixed to $|n| = |k| = 1$, and $e_r = \kappa = \beta = 1$.

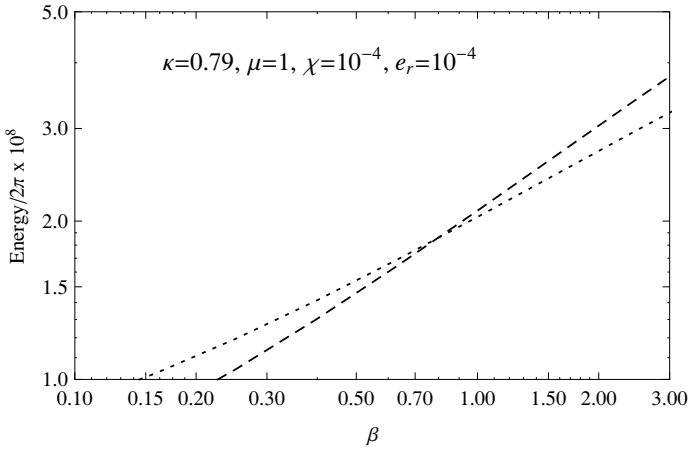

Figure 4. For e_r and χ very small the critical point does not change with respect to the case without mixing. Dashed lines correspond to the energy of a configuration $(2, 2)$ while dotted ones correspond to twice the energy of configuration $(1, 1)$.

We again chose to study the energy of a (2,2) vortex and compare it with twice the energy of a (1,1) vortex. We show in figures 4–5 the energy as a function of β for $e_r > 0$ (i.e. when both coupling constants have the same sign). Figure 4 shows that for e_h and χ very small ($e_h = \chi = 10^{-4}$) the critical stability point does not change with respect to the case without mixing. In contrast, when e_h grows beyond the value $e_h = 1$, the critical point moves to the right, as can be seen in figure 5 for $e_h = 10, 20$. Thus, as it was to be expected, only for large hidden gauge coupling charges vortex stability is significantly affected.

In the case $\operatorname{sign} e \neq \operatorname{sign} e_h$ (e.g. $e_r = -1$), interesting phenomena take place for a suitable choice of the remaining parameters. To see this let us consider a $\mathcal{CP}$ transformation of one of the fields, say $\tilde{G}_\mu \equiv \mathcal{CP}(G_\mu) = -G_\mu$ and choose $\tilde{G}_\mu = A_\mu$. Then, it is possible to get a cancelation of the kinetic terms for both vector fields when the physical parameters

JHEP12(2014)011

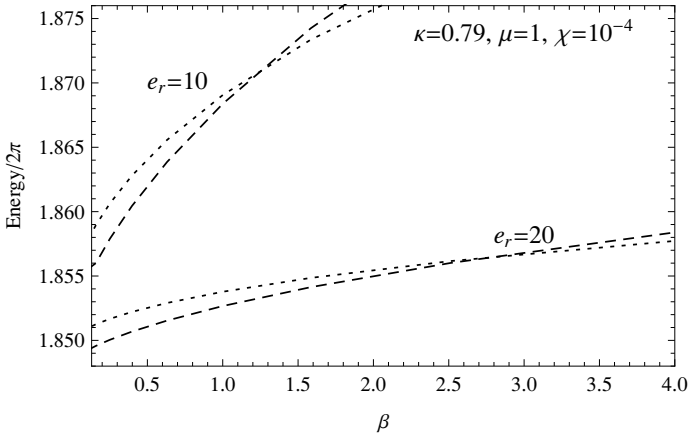

Figure 5. For large e_r and χ very small the critical point moves to the right with respect to the case without mixing. Dashed lines correspond to the energy of a configuration $(2, 2)$ while dotted ones correspond to twice the energy of configuration $(1, 1)$.

are chosen to be $\chi = \mu = 1$.[2] One could think of the above situation as describing a mixing between a gauge field from the visible sector and an anti-hidden gauge field from the hidden sector (of course this requires a definition of hidden field's antiparticles).

Now, when the gauge field kinetic terms cancel out, the field equation for the visible gauge field (which is identical to the CP transformed hidden one), reduces to

$$ie\phi^*(\partial^\mu - ieA^\mu)\phi = 0, \tag{4.3}$$

so that just using the scalar field ansatz (2.11) one has, from the angular equation

$$(\partial_\varphi - ieA_\varphi)\phi = i\rho(r)(n - eA_\varphi) = 0, \tag{4.4}$$

leading to

$$A_\varphi = \frac{n}{r} = \tilde{G}_\varphi. \tag{4.5}$$

The singularity at the origin of both fields shows that - in the case of study - there are no regular gauge field solutions. Note that this singular solution for the gauge fields has been obtained without any reference to the scalar fields radial solution $\rho(r)$, since the corresponding field equation is completely decoupled from the gauge field and depends only on the symmetry breaking potential. The only remnant of the gauge-scalar field interaction is the winding number n appearing in eq. (4.5) because of the phase in the scalar field ansatz.

If one inserts the solution (4.5) in field equation for the Higgs scalar,

$$D_\mu D^\mu \phi = \frac{\delta V[\phi]}{\delta \phi^*}, \tag{4.6}$$

one just gets

$$D_r D^r \phi = \frac{\delta V[\phi]}{\delta \phi^*}, \tag{4.7}$$

[2]Note the condition $|\chi| < 1$, previously found from asymptotic consistence does not hold in the present case.

JHEP12(2014)011

or, since $A_r = 0$

$$\rho(r)'' + \frac{1}{r}\rho' - \frac{\kappa^2}{2}(\rho^2 - 1)\rho = 0. \tag{4.8}$$

(The same result can be obtained by making $\alpha = 1$ in eq. (2.18)).

Comparing eq. (4.8) with the one corresponding to global vortices (see for example [21, 22]), one can see that the only difference between the two is that since there is no gauge field in the global U(1), its radial scalar field equation contains extra term proportional to n^2 which in our model's equation is canceled precisely by the contribution of A_φ. Precisely, due to the presence of this n^2 term, the global vortex energy diverges logarithmically [20].

To see whether there is any energy divergence in our case we insert ansatz (4.1), and the value of A_φ given in (4.5) in the energy per unit of length given by (2.8). We get (for $n = 1$)

$$\frac{E}{\phi_0^2 \ell} = 2\pi \left(\frac{1}{8} + \frac{89\kappa^2}{1152\mu^2} \right). \tag{4.9}$$

Hence, for any value of the variation parameter μ, the above expression is finite. Now the minimum value of the energy corresponds to $\mu \to \infty$, so that ρ becomes trivial, $\rho = 1$, and $\phi = \phi_0 e^{in\varphi}$, an ill-defined expression at the origin. Thus, the energy per unit of length vanishes, and no regular non-trivial vortex solution therefore exist. The same conclusion holds for arbitrary value n. This result could have been obtained just using the ordinary Bogomolny equations and replacing $\alpha(r) = 1$, which forces $\rho = 1$.

Another interesting result correspond to the case $e_r = -1$. Indeed, choosing the ansatz's radial functions $\gamma(r) = \alpha(r)$ and $\mu = \chi \to 1$, a cancellation of the kinetic terms for gauge fields γ and α also takes place. Moreover, once again a singular solutions for the gauge fields exist but consistency requires in this case an inverted magnetic flux condition imposing $n = -k$.

4.4 Radial dependence of fields

In order to discuss radial fields profiles and their dependence on the free parameters of the theory we shall follow two different numerical approaches: namely the variational approach already discussed and a shooting method.

We start by varying the kinetic mixing parameter χ, setting the rest of the parameters to unity, $e_r = \beta = \kappa = \mu = 1$ and the winding numbers $k = n = 1$ so that visible and hidden fields are indistinguishable.

In figure 6(a) we plot the visible magnetic fields obtained using the shooting method as a function of r for several values of the kinetic mixing parameter χ. We can conclude that increasing χ makes the magnitude of the magnetic field to decrease, thus lowering the visible magnetic energy.

Figure 6(b) shows the hidden magnetic field as a function of r for several values of χ, using the shooting solution. Since the visible and hidden fields are indistinguishable, we obtain the same profile as the visible field. In figure 7 we compare the visible and hidden scalar fields as a function of r for several values of χ. From this graph we conclude that as the kinetic mixing parameter increases, the field reduces its asymptotic value.

JHEP12(2014)011

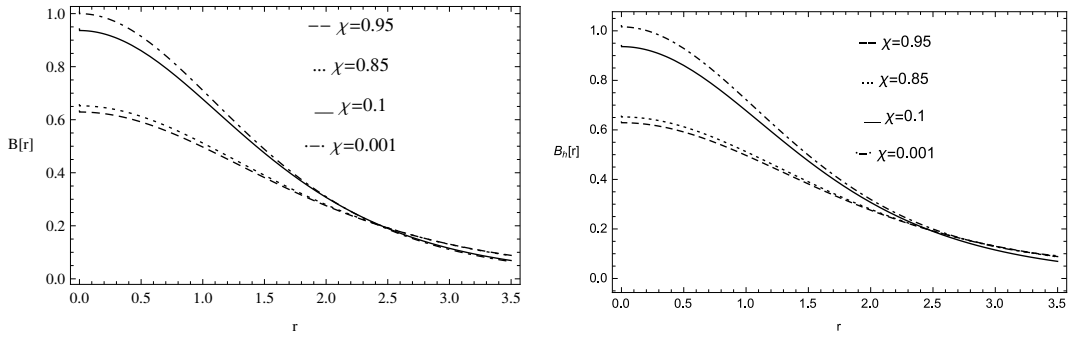

(a) (b)

Figure 6. (a): visible magnetic field profiles for several values of the kinetic mixing parameter χ. (b): hidden magnetic field as a function of the kinetic mixing parameter χ. The rest of the parameters have been fixed as $e_r = \mu = \kappa = \beta = 1$, and the winding numbers $n = k = 1$.

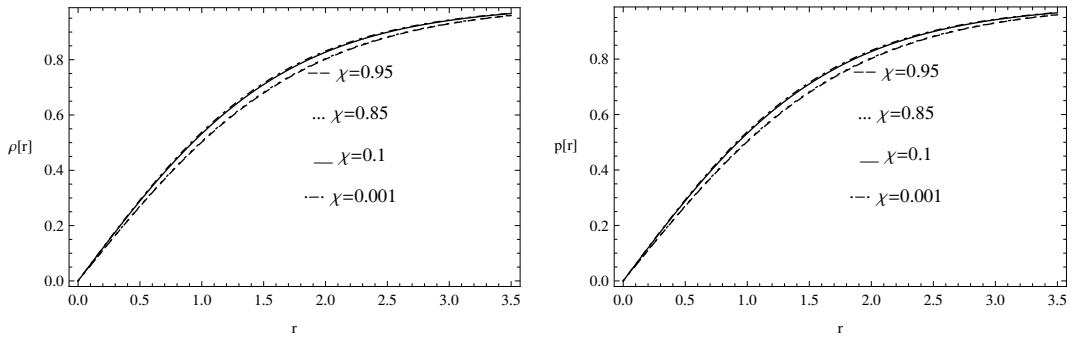

(a) (b)

Figure 7. (a): visible Higgs field profiles for several values of the kinetic mixing parameter χ. (b): hidden Higgs field as a function of the kinetic mixing parameter χ. The rest of the parameters have been fixed as $e_r = \mu = \kappa = \beta = 1$, and the winding numbers $n = k = 1$.

Further, we have studied the behavior of the solution under the change of the mass ratio parameter μ which has phenomenological relevance. Note that for fixed $m_A = 1$, increasing μ is equivalent to make the vacuum value of the hidden Higgs field larger than the visible one.

We have again taken $e_r = \beta = \kappa = 1$, and a small value for $\chi = 10^{-4}$. The results we report were obtained using the variational approach, since for large μ it is more appropriate than the shooting method. We plot in figure 10 the visible magnetic fields as a function of r for several values of μ. The plot suggests that when $\mu \geq 10$ the visible magnetic field changes, both in magnitude and penetration depth. This interesting result shows that a shorter range of the hidden field enforces the shortening of the visible range showing that non linear terms of the slowly decaying field affects the $\mu \lesssim 5$ range, where both the shooting and the variational methods are both applicable their results coincide showing that the visible magnetic field has the same behavior as the one where the visible sector has no mixing with a hidden sector.

JHEP12(2014)011

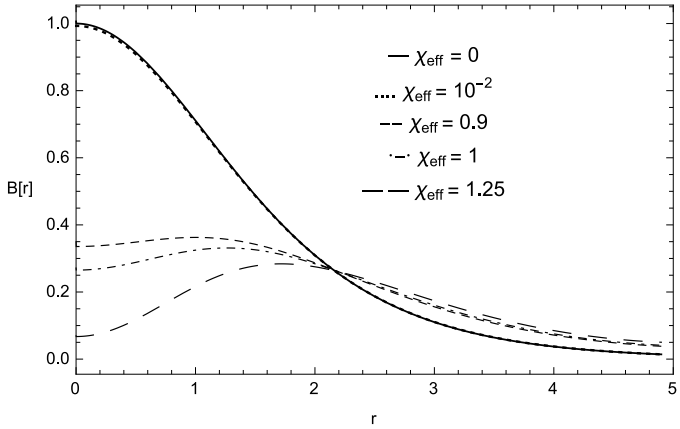

Figure 8. Visible magnetic field profile for different values of the effective kinetic mixing $\chi_{\text{eff}} = \chi/e_r$. For all curves, the kinetic mixing is fixed to $\chi = 10^{-5}$. The rest of the parameters remain as $\mu = \kappa = \beta = 1$, with winding numbers $n = k = 1$.

We have also studied the field behavior under changes in χ/e_r. From the analysis of the previous sections one can see that this ratio can be regarded as an effective kinetic mixing which we shall call $\chi_{\text{eff}} \equiv \chi/e_r$. In particular, using χ_{eff} instead of just χ allows to consider more realistic values of the latter.

The profiles of the visible magnetic field for different values of χ_{eff} are shown in figure 8. Keeping χ fixed to $\chi = 10^{-5}$, we considered different values e_r. Our results show that for a small χ_{eff}, ($e_r \gg \chi$) the magnetic field shows no departure from the behavior corresponding to the absence of kinetic gauge mixing mixing with a hidden sector. However, as χ_{eff} grows, (*i.e.* $e_r \lesssim \chi$) the magnetic field decreases but it has a slower decay as r grows. For the curves of figure 8 we have fixed the rest of the physical parameters to unity. Note that a value of $\chi_{\text{eff}} > 1$ can be achieved by choosing small values of the kinetic mixing, for instance $\chi = 10^{-7}$ and $e_r = 10^{-8}$.

4.5 Vortex decay into elementary configurations

Vortices with winding numbers (n, k) could be unstable and decay into lower energy configurations, when available, as it is the case in the ordinary Abelian Higgs model [11]. Indeed, in the absence of the hidden sector, the energy density in the type-II superconductivity vortex regime ($\kappa > 1$) is proportional to the winding number squared, say n^2. Thus, a vortex with winding number $n = 2$, will decay into two vortices of winding number $n = 1$. We already studied the stability of the vortices on general grounds in sections 4.2 and 4.3.

When the mixing with the hidden sector is considered, the energy is no longer proportional to the two available winding numbers, n^2, k^2, but will also depend on the contribution of the mixing term, which is related to winding number n and k through the field strengths and also depends on the values of parameters χ and e_r. In fact, we have seen in section 3.2 that vortex decay depends crucially on the sign of χ.

We shall consider two types of elementary vortex configurations: the $(1, 0)$ one carrying just one unit of visible magnetic flux and the $(0, 1)$ carrying instead just one unit of hidden magnetic flux. Then, starting with an (n, k) configuration we shall analyze under which

JHEP12(2014)011

	$\kappa=\beta=0.6$		$\kappa=\beta=0.8$	
χ	(2,2)	$2(0,1)+2(1,0)$	(2,2)	$2(0,1)+2(1,0)$
10^{-6}	3.2007	3.3100	3.7194	3.7163
10^{-3}	3.2016	3.3100	3.7207	3.7164
10^{-1}	3.2806	3.3034	3.8380	3.7088
0.5	3.5569	3.1277	4.2366	3.5060

Table 1. Energy of the $(2,2)$ configuration (second and forth columns) and that of the $2(0,1)+2(1,0)$ (third and fifth columns) for different values of the kinetic mixing parameter χ, and two different values of the Landau parameters $\kappa=\beta$. The rest of the physical parameters have been fixed to $e_r=\mu=1$.

conditions such configuration could decay into one with n elementary vortices of type (1,0) and k elementary vortices vortices $(0,1)$. Let us consider for definiteness the unbroken symmetry case discussed in our previous section. Taking for instance $\phi=0,\kappa=0$ one can construct a $k(1,0)$ configuration with k spatially superimposed hidden vortices of unit flux. Then, a vortex configuration of the type $n(1,0)+k(0,1)$ can be formed by considering this configuration and one where where the role of visible and hidden fields is inverted and k is replaced by n.

We illustrate the decay from the (n,k) configuration as described above in table 1 by comparing the energies of the $(2,2)$ configuration with that of the $2(0,1)+2(0,1)$ one, for different values of χ and Landau parameters, κ,β. As we can see, for small values ($\chi\sim 10^{-6}$) the decay of the configuration $(2,2)$ into the elementary ones takes place approximately at the critical value of the Landau parameters if the mixing were absent, that is, for $\kappa=\beta\sim 0.8$. Now, as the mixing parameter grows, the decay takes place at lower and lower values of the Landau parameters. For instance, for $\chi\geq 0.5$ the decay of the vortex $(2,2)$ already occurs at $\kappa=\beta=0.6$.

Let us note that one can reach the same conclusion by varying e_r while keeping the kinetic mixing small, as discussed when we studied the radial fields profiles in terms of the effective mixing parameter χ_{eff}. Note that for phenomenologically acceptable very small kinetic mixing parameter ($\chi\sim 10^{-6}$ or lower), the effect described above takes place when the hidden gauge coupling constant is very small, $e_h/e\lesssim 10^{-6}$.

Finally, we have investigated the effect of changes of the vector fields masses in the decay scenario. In table 2 the energies of a $(2,2)$ with a $2(0,1)+2(0,1)$ configuration are compared for several values of the mass ratio μ and for two different points of (κ,β). One can see that increasing μ does not affect the stability of the vortices.

5 The fields behavior in connection with superconductivity

In view of the connection between the Landau-Ginzburg phenomenological theory for superconductors [23] and the Abelian Higgs Model, superconductivity is a possible arena to test whether the mixing between the hidden and visible sectors could have a phenomeno-

JHEP12(2014)011

	$\kappa=\beta=0.77$		$\kappa=\beta=0.8$	
μ	(2,2)	$2(0,1)+2(1,0)$	(2,2)	$2(0,1)+2(1,0)$
10^{-3}	1.82266	1.85818	1.85975	1.85818
0.1	1.84087	1.87647	1.87832	1.87676
1.0	3.64538	3.68768	3.71954	3.71635
20	730.8801	733.6594	750.5002	745.1293

Table 2. Energy of the $(2,2)$ configuration (second and fourth columns) and that of the $2(0,1)+2(1,0)$ (third and fifth columns) for different values of the ratio of vector field masses, μ, and two different values of the Landau parameters $\kappa=\beta=\{0.77,0.8\}$. The rest of the physical parameters have been fixed to $e_r=1$ and $\chi=10^{-4}$.

logical impact. In this section we intend to give a brief and qualitative discussion on this issue.

If one looks for measurable quantities that may have been affected by the gauge mixing in the superconductivity context, the scale lengths in the theory are natural the candidates to analyze. In ordinary superconductivity (i.e., in the absence of a hidden sector) there are two characteristic lengths. One of them is the penetration depth of the external magnetic field, ℓ. In the language we have been using, it is given by the inverse of the effective mass of the gauge field, thus $\ell=m_A^{-1}$. The other one is the characteristic length for the Cooper pairs, known as the *coherence length*, ξ which in our notation would be $\xi=m_\varphi^{-1}$. These two lengths can be combined into one via the Landau parameter, defined in our model as $\kappa=\ell^2/\xi^2$. Thus, within a phenomenological Ginzburg-Landau approach, there is only one free parameter, the Landau parameter which, after redefinitions of section 2, is given by $\kappa=\sqrt{2\lambda}/e$.

The results obtained in subsection 4.4 imply that when χ (or $\chi_{\rm eff}$) approaches unity the visible fields get greatly modified, as it happens for large values of the gauge boson masses ratio of μ. This means that depending on the values of physical parameters $(\mu,e_r,\chi,\kappa,\beta)$ the energy of a superconductor can get modified, thus affecting the superconducting sample behavior, in particular the exclusion of the magnetic field from it.

In order to analyze this issue we shall study the energy density behavior as a function of r in the context of superconductivity, when a mixing of visible photons with massive hidden photons through the kinetic mixing is present. We shall assume for simplicity that energy density in the superconductor sample is governed - within the Ginzburg-Landau approach - by a the usual free energy density, just composed of the visible magnetic field, the kinetic energy of the super current and the condensation energy of the Cooper pairs. The existence of a hidden sector will be taken into account by inserting in such free energy the solutions obtained by the minimization of the complete visible-hidden model, eq. (2.5). Then, the free energy density in the superconductor is taken as

$$\mathcal{F}_s^{visible}=\frac{B^2}{2}+\frac{1}{2}|\partial_i\phi-iA_i\phi|^2+\frac{\kappa^2}{8}\left(|\phi|^2-1\right)^2, \tag{5.1}$$

JHEP12(2014)011

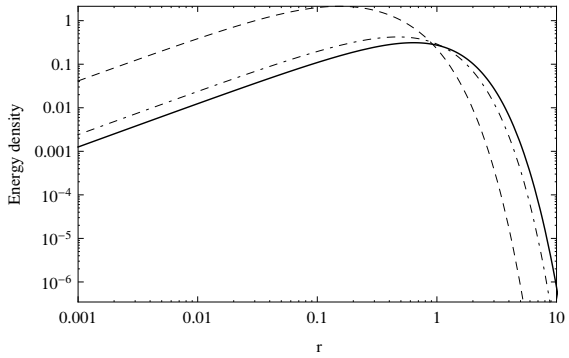

Figure 9. Energy density profiles for several values of μ (we have set $\kappa = 1$). The continuous solid line corresponds to the energy in the case of no mixing with a hidden sector. The dot-dashed line corresponds to $\mu = 15$ and the dashed line corresponds to $\mu = 20$. Thus, when the mass of the hidden gauge boson grows significantly from unity, the energy density of the superconductor departs from the value of the usual Ginzburg-Landau theory. The rest of the parameters have been chosen as: $\beta = \kappa = e_r = 1$, and $\chi = 10^{-4}$.

χ	$\sigma/2\pi$
10^{-3}	0.000003
10^{-2}	0.000036
10^{-1}	0.000709
0.85	0.003882
0.95	0.04066

Table 3. Surface energy for different values of the kinetic mixing parameter. As χ increases, the surface energy also increases. The remaining parameters have been fixed as $\kappa = \beta = e_r = \mu = 1$.

Note that with our conventions the *Landau parameter* is just κ and the Bogomolny point is $\kappa = 1$.

We show in figure 9 the energy density, (5.1) as a function of r for several values of the hidden vector field mass. The continuous solid line in the figure corresponds to the case of an ordinary superconductor (i.e. in the absence of a hidden sector). As we can see, when the parameter μ is small ($\mu \lesssim 15$) there is no appreciable change of the free energy compared to the one where there is no mixing with a hidden sector. As this parameter grows, we observe a departure from the ordinary superconductor curve. This result agrees with those reported in section 4. For high values of μ the visible magnetic field increases its amplitude, thus increasing the magnetic energy, but its penetration depth decreases. A similar conclusion should be reached by considering the energy density for different values of χ_{eff}.

The surface energy between a normal and superconducting samples is a relevant quantity in superconductivity since its sign unequivocally defines the transition between type-I and type-II superconductivity. The minimum of the surface energy occurs at the point

JHEP12(2014)011

χ_{eff}	$\sigma/2\pi$
0.01	0.000242
0.1	0.007925
0.9	0.058660
1.0	0.069072
1.25	0.102120

Table 4. Surface energy for different values of the effective kinetic mixing parameter. As χ_{eft} increases, the surface energy also increases. For all the values shown here we have considered a kinetic mixing of $\chi = 10^{-5}$. The remaining parameters have been fixed as $\kappa = \beta = \mu = 1$.

where the free energy gets its minimum (where the Bogomolny bound is saturated), which in a normal Nielsen-Olesen vortex, with dimensionless variables, is $\kappa = 1$.

We have numerically studied the two dimensional surface energy σ associated to the visible sector of our model, given by

$$\sigma = 2\pi \int_0^\infty \left(\frac{1}{2} \left(B(r) - \frac{\kappa}{2} \right)^2 - \frac{\kappa^2}{8} \rho(r)^4 \right) r dr \tag{5.2}$$

We see from this equation that σ vanishes when $B(r) = \kappa/2 \left(1 + \rho(r)^2\right)$, which is indeed the Bogomolny equation for the ordinary Abelian Higgs model holding when $\kappa = 1$.

As stated above, the visible magnetic and scalars fields in eq. (5.2) correspond to the solutions of the complete set (2.16)–(2.19) that we found using an improved shooting method in order to refine accuracy of the calculation. To determine how the surface energy measured in experiment could be affected by the existence of a hidden sector, we have varied the free parameters of our model and made use of the equation for the surface energy. We show in table 3 the value of the surface energy when $\kappa = 1$ for different values of the parameter χ. The rest of the phenomenological parameters were fixed to $\beta = e_r = \mu = 1$. We clearly see that increasing the value of χ makes the surface energy at $\kappa = 1$ to grow. This result can be interpreted as a shift in the value of the limiting point between type-I and type-II superconductivity supporting our previous statement on the non-existence of first order Bogomolny equations.

From the experimental point of view such large values of the kinetic mixing parameter χ have been ruled out by experiments [13]. In view of this, we have computed the surface energy in terms of the *effective* kinetic mixing $\chi_{\text{eff}} \equiv \chi/e_r$. In this way we can consider more realistic values χ taking a small value for the hidden gauge coupling compared to the visible one. In table 4 we show the surface energy, eq. (5.2) for different values of the effective kinetic mixing. One can see that even for small kinetic mixing the surface energy now changes appreciably

Concerning the visible magnetic field profiles, the results plotted in figure 10 suggest that the point at which the surface energy vanishes also changes as μ grows significantly

JHEP12(2014)011

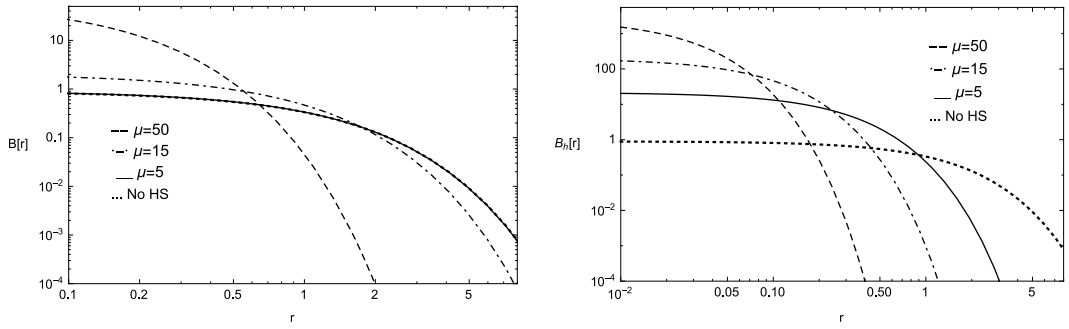

(a) (b)

Figure 10. (a): Visible magnetic field profiles for several gauge bosons masses, μ. (b): hidden magnetic field profiles for several values of μ. Both plots have been obtained using the variational method. The rest of the parameters have been fixed as $e_r = \kappa = \beta = 1$, $\chi = 10^{-4}$, and the winding numbers $n = k = 1$.

6 Summary and discussion

In this work we have analyzed a gauge theory with a visible and a hidden sector with dynamics governed by two Abelian Higgs Lagrangians coupled through a gauge kinetic mixing. Imposing the usual cylindrically symmetric Nielsen-Olesen ansatz for gauge and scalar fields we have arrived to a system of 4 coupled radial equations which we have solved numerically.

We have started studying the case in which the U(1) gauge symmetry is unbroken in one of the two sectors. This was achieved by not including in the Lagrangian the corresponding complex scalar. We found that even in this case the kinetic gauge mixing forces the existence of vortex configurations also in the unbroken sector with associated magnetic field decaying exponentially at infinity with the same length as the one in the broken symmetry sector.

Interestingly, always in the case in which one U(1) symmetry is unbroken, gauge and scalar self-interaction coupling constants satisfy a relation which depends on the value of gauge mixing parameter χ and first order Bogomolny equations exist in the broken sector. The fact that the two fields strengths are proportional (with a proportionality factor $(e\chi/e_h)$) explains why both magnetic fields have the same exponential decay. This is a relevant result that could be in principle exploited considering for instance primordial magnetic fields generation by dark superconducting strings in the early universe [19].

Concerning the case in which both U(1) gauge symmetries are broken, we have found that the relevant parameters controlling stability are χnk (with n and k the units of magnetic flux) and the ratio of the gauge couplings $e_r = e_h/e$. Our numerical analysis shows that for growing values of $\chi nk > 0$ and $e_r > 0$, the instability regime starts at lower values of the hidden sector of the Landau parameter. If χ is instead positive but $nk < 0$ with e_r positive we find that the energy gets reduced as the parameter χ grows, the opposite of the $\chi nk > 0$ case.

We also studied the dependence of the solutions on the gauge coupling constants ratio e_r. To this end we considered the case of small $\chi \sim 10^{-4}$ so as to detect the individual

JHEP12(2014)011

dependence on e_r. When $e_r > 0$, for very small values of e_r ($e_r = 10^{-4}$) the critical stability point does not change significantly compared to the case with no mixing. In contrast, when $e_r > 1$ the decay critical stability point moves to the right as e_r grows.

Interesting phenomena take place when $\operatorname{sign} e \neq \operatorname{sign} e_h$ (i.e. $e_r < 0$) together with suitable choices of the remaining parameters. In particular if the $\mathcal{CP}$ transformed hidden gauge field is equal to the visible one, $\mathcal{CP}(G_\mu) = A_\mu$, the kinetic terms for both vector fields cancel out for $\chi \to 1$ and $m_A = m_G$. This identification can be interpreted in terms of a mixing between a photon from the visible sector and an anti-hidden photon from the hidden sector (of course this requires a definition of hidden field's antiparticles). Being the gauge kinetic terms absent, one finds a solution of the form $\phi = \phi_0 \exp(in\varphi)$ and $A_\varphi = n/r$. That is, both fields are singular at the origin but the singularities cancel out when computing the energy per unit length.

We have found that both hidden and visible magnetic fields reduce their magnitude when χ or χ_{eff} approaches unity. In respect to changes in μ, the variational method shows observable effects in the visible magnetic fields when $\mu \gtrsim 15$. Concerning the hidden magnetic field, it grows significantly for $\mu \gtrsim 1$.

Concerning the decay of (n, k) vortices we have studied the case in which the final configuration is a combination of $n(1, 0)$ and $k(0, 1)$ elementary vortices. The conclusion is that as the gauge mixing parameter grows, the decay takes place at lower and lower values of the hidden Landau parameter with the visible one is fixed. The same holds if one varies χ_{eff} or $1/e_r$. Using a phenomenologically acceptable kinetic mixing parameter ($\chi \sim 10^{-6}$) the effect described above takes place when the hidden gauge coupling constant satisfies $e_h/e \lesssim 10^{-6}$.

We have also presented a qualitative discussion of the results from previous sections in connection with superconductivity. As expected, for small χ the results remain unchanged with respect to the case in which no hidden sector is present. We have shown that the mass ratio μ and effective gauge kinetic mixing χ_{eff} are the relevant parameters to study the hidden sector effect on a superconductor sample. Concerning the former, we found that the energy density grows when μ increases, but the effective penetration length is reduced. In the normal superconducting theory the surface energy is zero at the Bogomolny point $\kappa = 1$. However, in the presence of a gauge mixing, when χ or χ_{eff} approach unity the surface energy changes its behavior and does not vanish for $\kappa = 1$.

We conclude that in view of the very rich structure of the vortex solution space that we have found, it would be worthwhile to analyze the role of the vortex configurations in cosmology, hidden photon search and supersymmetric extensions. We expect to discuss these issues in a future work.

Acknowledgments

P.A. was supported by FONDECYT project 11121403 and Anillo ACT 1102. F.A.S is financially supported by CONICET, ANPCIT, UNLP and CICBA grants

We are specially thankful of E. Moreno for his useful comments and help in the numerical calculations, J. Jaeckel, for reading the manuscript and for his valuable comments,

JHEP12(2014)011

J. Gamboa for his suggestion and encouragement to look into this subject, and A. Ringwald and J. Redondo for their participation in earlier stages of this work. We are also thankful of G. Duering, G. Lozano and E. Muñoz for discussions and comments.

A Asymptotic behavior of the radial fields

We find numerical solutions of the radial equations eqs. (2.16)–(2.19) by implementing a shooting method to match the solutions of these equations in the limit $r \to \infty$. In order to find the analytical asymptotic solutions of these equations, we start by defining the functions $\tilde{\alpha} = \alpha - 1$ and $\tilde{\gamma} = \gamma - 1$, $\tilde{\rho} = \rho - 1$, $\tilde{p} = p - \frac{\mu}{e_r}$ such that in the limit $r \to \infty$, they all satisfy

$$\begin{aligned} \lim_{r\to\infty} \tilde{\rho}(r) &= 0\,, & \lim_{r\to\infty} \tilde{p}(r) &= 0. \\ \lim_{r\to\infty} \tilde{\alpha}(r) &= 0\,, & \lim_{r\to\infty} \tilde{\gamma}(r) &= 0. \end{aligned} \tag{A.1}$$

With these redefinitions, eqs. (2.16)–(2.19) take in the asymptotic limit the form

$$\left[r\frac{d}{dr}\left(\frac{1}{r}\frac{d}{dr}\right)\right]\left(n\tilde{\alpha} + \frac{k}{e_r}\chi\tilde{\gamma}\right) - n\tilde{\alpha} = 0, \tag{A.2}$$

$$\left[r\frac{d}{dr}\left(\frac{1}{r}\frac{d}{dr}\right)\right]\left(\frac{k}{e_r}\tilde{\gamma} + n\chi\tilde{\alpha}\right) - \frac{k}{e_r}\mu^2\tilde{\gamma} = 0, \tag{A.3}$$

$$\tilde{\rho}'' + \frac{\tilde{\rho}}{r} - \kappa^2\tilde{\rho} = 0, \tag{A.4}$$

$$\tilde{p}'' + \frac{\tilde{p}}{r} - (\beta\mu)^2\,\tilde{p} = 0. \tag{A.5}$$

$$\tag{A.6}$$

The solutions for $\tilde{\rho}$ and $\tilde{p}$ are

$$\tilde{\rho}(r) = D_1 K_0(\kappa r) + D_2 I_0(\kappa r), \tag{A.7}$$

$$\tilde{p}(r) = E_1 K_0(\mu\beta r) + E_2 I_0(\mu\beta r). \tag{A.8}$$

Making $n\tilde{\alpha} \to \tilde{\alpha}$ and $k/e_r\tilde{\gamma} \to \tilde{\gamma}$ eqs.(A.2)–(A.3) become

$$\left[r\frac{d}{dr}\left(\frac{1}{r}\frac{d}{dr}\right)\right](\tilde{\alpha} + \chi\tilde{\gamma}) - \tilde{\alpha} = 0, \tag{A.9}$$

$$\left[r\frac{d}{dr}\left(\frac{1}{r}\frac{d}{dr}\right)\right](\tilde{\gamma} + \chi\tilde{\alpha}) - \mu^2\tilde{\gamma} = 0, \tag{A.10}$$

which can be combined into the equation

$$\left[r\frac{d}{dr}\left(\frac{1}{r}\frac{d}{dr}\right)\right](\tilde{\alpha}\,(A + \chi B) + \tilde{\gamma}\,(B + \chi A)) = A\tilde{\alpha} + B\mu^2\tilde{\gamma}, \tag{A.11}$$

where A, B are arbitrary constants. We now introduce C

$$A + \chi B = CA, \tag{A.12}$$

$$B + \chi A = CB\mu^2, \tag{A.13}$$

JHEP12(2014)011

and solve for A finding

$$\frac{A_\pm}{B} = \frac{\mu^2 - 1}{2\chi} \pm \frac{1}{2\chi}\sqrt{(1-\mu^2)^2 + 4\mu^2\chi^2}. \tag{A.14}$$

So that $C_\pm$ can be written as

$$C_\pm = \frac{1}{2\mu^2}\left(\mu^2 + 1 \pm \sqrt{(1-\mu^2)^2 + 4\mu^2\chi^2}\right). \tag{A.15}$$

With this eq. (A.11) becomes (for $\chi \neq 1$)

$$\left[r\frac{d}{dr}\left(\frac{1}{r}\frac{d}{dr}\right)\right] F_\pm(r) = \frac{1}{\sqrt{C_\pm}} F_\pm, \tag{A.16}$$

where the functions $F_\pm(r)$ are defined as

$$F_\pm(r) = \frac{A_\pm}{B}\tilde{\alpha} + \mu^2\tilde{\gamma}. \tag{A.17}$$

The solution of equation (A.16) is then

$$F_+(r) = A_1 r K_1\left(\frac{r}{\sqrt{C_+}}\right) + A_2 r I_1\left(\frac{r}{\sqrt{C_+}}\right), \tag{A.18}$$

$$F_-(r) = B_1 r K_1\left(\frac{r}{\sqrt{C_-}}\right) + B_2 r I_1\left(\frac{r}{\sqrt{C_-}}\right). \tag{A.19}$$

Form this result one gets $\tilde{\alpha}$ and $\tilde{\gamma}$ in the asymptotic limit $r \to \infty$

$$\tilde{\alpha} = n\frac{F_+ - F_-}{A_+/B - A_-/B}, \tag{A.20}$$

$$\tilde{\gamma} = \frac{k}{e_r}\frac{((A_-/B)F_+ - (A_+/B)F_-)}{\mu^2\,(A_+/B - A_-/B)}. \tag{A.21}$$

Now, in order to have exponential decays for the massive fields at $r \to \infty$ one should impose $C_\pm > 0$, which in turn implies

$$\left(1+\mu^2\right)^2 > \left(1-\mu^2\right)^2 + 4\mu^2\chi^2, \tag{A.22}$$

or

$$\chi^2 < 1. \tag{A.23}$$

This is an important result showing that in order to have finite energy vortex solutions parameter χ controlling the mixing between the visible and the hidden sectors should satisfy $|\chi| < 1$.

JHEP12(2014)011

References

[1] J. Jaeckel and A. Ringwald, *The low-energy frontier of particle physics*, *Ann. Rev. Nucl. Part. Sci.* **60** (2010) 405 [arXiv:1002.0329] [INSPIRE].

[2] A.E. Nelson and J. Scholtz, *Dark light, dark matter and the misalignment mechanism*, *Phys. Rev.* **D 84** (2011) 103501 [arXiv:1105.2812] [INSPIRE].

[3] P. Arias et al., *WISPy cold dark matter*, *JCAP* **06** (2012) 013 [arXiv:1201.5902] [INSPIRE].

[4] N. Arkani-Hamed, D.P. Finkbeiner, T.R. Slatyer and N. Weiner, *A theory of dark matter*, *Phys. Rev.* **D 79** (2009) 015014 [arXiv:0810.0713] [INSPIRE].

[5] L.B. Okun, *Limits of electrodynamics: paraphotons?*, *Sov. Phys. JETP* **56** (1982) 502 [*Zh. Eksp. Teor. Fiz.* **83** (1982) 892] [INSPIRE].

[6] B. Holdom, *Two* U(1)*'s and epsilon charge shifts*, *Phys. Lett.* **B 166** (1986) 196 [INSPIRE].

[7] T. Vachaspati, *Dark strings*, *Phys. Rev.* **D 80** (2009) 063502 [arXiv:0902.1764] [INSPIRE].

[8] B. Hartmann and F. Arbabzadah, *Cosmic strings interacting with dark strings*, *JHEP* **07** (2009) 068 [arXiv:0904.4591] [INSPIRE].

[9] Y. Brihaye and B. Hartmann, *The effect of dark strings on semilocal strings*, *Phys. Rev.* **D 80** (2009) 123502 [arXiv:0907.3233] [INSPIRE].

[10] J.M. Hyde, A.J. Long and T. Vachaspati, *Dark strings and their couplings to the standard model*, *Phys. Rev.* **D 89** (2014) 065031 [arXiv:1312.4573] [INSPIRE].

[11] L. Jacobs and C. Rebbi, *Interaction energy of superconducting vortices*, *Phys. Rev.* **B 19** (1979) 4486.

[12] M. Cicoli, M. Goodsell, J. Jaeckel and A. Ringwald, *Testing string vacua in the lab: from a hidden CMB to dark forces in flux compactifications*, *JHEP* **07** (2011) 114 [arXiv:1103.3705] [INSPIRE].

[13] R. Essig et al., *Working group report: new light weakly coupled particles*, arXiv:1311.0029 [INSPIRE].

[14] H.J. de Vega and F.A. Schaposnik, *A classical vortex solution of the abelian Higgs model*, *Phys. Rev.* **D 14** (1976) 1100, reprinted in *Solitons and particles*, C. Rebbi and G. Soliani eds., World Scientific, Singapore (1984), [INSPIRE].

[15] E.B. Bogomolny, *Stability of classical solutions*, *Sov. J. Nucl. Phys.* **24** (1976) 449, reprinted in *Solitons and particles*, C. Rebbi and G. Soliani eds., World Scientific, Singapore (1984), [*Yad. Fiz.* **24** (1976) 861] [INSPIRE].

[16] H.B. Nielsen and P. Olesen, *Vortex line models for dual strings*, *Nucl. Phys.* **B 61** (1973) 45, reprinted in *Solitons and particles*, C. Rebbi and G. Soliani eds., World Scientific, Singapore (1984), [INSPIRE].

[17] F. Brummer and J. Jaeckel, *Minicharges and magnetic monopoles*, *Phys. Lett.* **B 675** (2009) 360 [arXiv:0902.3615] [INSPIRE].

[18] F. Brummer, J. Jaeckel and V.V. Khoze, *Magnetic mixing: electric minicharges from magnetic monopoles*, *JHEP* **06** (2009) 037 [arXiv:0905.0633] [INSPIRE].

[19] T. Vachaspati, *Magnetic fields from cosmological phase transitions*, *Phys. Lett.* **B 265** (1991) 258 [INSPIRE].

[20] C.T. Hill, H.M. Hodges and M.S. Turner, *Bosonic superconducting cosmic strings*, *Phys. Rev.* **D 37** (1988) 263.

JHEP12(2014)011

[21] A. Vilenkin and A.E. Everett, *Cosmic strings and domain walls in models with Goldstone and pseudo-Goldstone bosons*, *Phys. Rev. Lett.* **48** (1982) 1867 [INSPIRE].

[22] A.A. Vilenkin and E.P.S. Shellard, *Cosmic strings and other topological deffects*, Cambridge University Press, Cambridge U.K. (1994).

[23] V.L. Ginzburg and L.D. Landau, *On the theory of superconductivity*, *Zh. Eksp. Teor. Fiz.* **20** (1950) 1064 [INSPIRE].

JHEP12(2014)011